IOP Publishing Journal of Physics: Condensed Matter
J. Phys.: Condens. Matter **32** (2020) 325402 (7pp) https://doi.org/10.1088/1361-648X/ab7f04

Coupling between phase transitions and glassy magnetic behaviour in Heusler alloy $Ni_{50}Mn_{34}In_8Ga_8$

Le Zhang[1,2,3], Xiaojie Lou[1], Chao Zhou[4], Sen Yang[4], Xiaobing Ren[1,5,6], Danyang Wang[3,6] and Michael A Carpenter[2,6]

[1] Frontier Institute of Science and Technology and State Key Laboratory for Mechanical Behavior of Materials, Xi'an Jiaotong University, Xi'an, 710049, People's Republic of China
[2] Department of Earth Sciences, University of Cambridge, Downing Street, Cambridge, CB2 3EQ, United Kingdom
[3] School of Materials Science and Engineering, The University of New South Wales, Sydney, NSW 2052, Australia
[4] School of Science, MOE Key Laboratory for Nonequilibrium Synthesis and Modulation of Condensed Matter, Xi'an Jiaotong University, Xi'an 710049, People's Republic of China
[5] Center for Functional Materials, National Institute for Materials Science, Tsukuba 305-0047, Ibaraki, Japan

E-mail: Ren.xiaobing@xjtu.edu.cn, dy.wang@unsw.edu.au and mc43@esc.cam.ac.uk

Received 19 December 2019, revised 18 February 2020
Accepted for publication 11 March 2020
Published 14 May 2020

Abstract

The transition sequence in the Heusler alloy $Ni_{50}Mn_{34}In_8Ga_8$ has been determined from measurements of elasticity, heat flow and magnetism to be paramagnetic austenite → paramagnetic martensite → ferromagnetic martensite at ∼335 and ∼260 K, respectively, during cooling. The overall pattern of elastic stiffening/softening and acoustic loss is typical of a system with bilinear coupling between symmetry breaking strain and the driving structural/electronic order parameter, and a temperature interval below the transition point in which ferroelastic twin walls remain mobile under the influence of external stress. Divergence between zero-field-cooling and field-cooling determinations of DC magnetisation below ∼220 K indicates that a frustrated magnetic glass develops in the ferromagnetic martensite. An AC magnetic anomaly which shows Vogel–Fulcher dynamics in the vicinity of ∼160 K is evidence of a further glassy freezing process. This coincides with an acoustic loss peak and slight elastic stiffening that is typical of the outcome of freezing of ferroelastic twin walls. The results suggest that local strain variations associated with the ferroelastic twin walls couple with local moments to induce glassy magnetic behaviour.

Keywords: Heusler alloy, phase transitions, elasticity

Supplementary material for this article is available online

(Some figures may appear in colour only in the online journal)

1. Introduction

Phase transformations in ferroic materials, i.e. ferroelectrics, ferroelastics and ferromagnets, have been intensively studied in recent years because of their particular structure/property relationships which arise as a consequence of order parameter

[6] The authors to whom any correspondence should be addressed.

instabilities in response to conjugate fields [1–3]. As an important group of ferroic materials, Heusler ferromagnetic shape memory alloys have attracted particular interest due to their giant magnetostrain, ∼3%–9.5%, which can be induced by the phase transformation between austenite and martensite [4] or the reorientation of ferromagnetic martensitic variants under applied field [5]. In addition, a large inverse magnetocaloric effect of ∼−7 K has been reported in the Ni–Mn–In system under a magnetic field of 6 T [6].

These promising multifunctional properties essentially depend on the nature and strength of strain/order parameter coupling and the mobility of ferroelastic domain walls [1]. The temperature dependence of elastic constants, magnetization and elastic damping properties of Ni–Mn–In and Ni–Mn–Ga based Heusler alloys have already been studied to some extent [7, 8], but those of polycrystalline NiMnIn–xNiMnGa alloys have not and should be much more complex than the two end members. Insights into strain-related phenomena at phase transitions of materials are provided by the associated variations of elastic constants. Resonant ultrasound spectroscopy (RUS) has turned out to provide a convenient tool for characterizing both the strength of strain/order parameter coupling, and the relaxation dynamics of ferroelastic domain walls or other defects at frequencies in the vicinity of ∼1 MHz [1, 7–13]. Integration of AC and DC magnetization data with results from RUS measurements then allows strain relaxation and magnetic dynamics to be characterized properly. This combined experimental approach should shed light on the full physical picture of magnetoelastic transitions in Heulser alloys, in particular for the NiMnIn–xNiMnGa alloys.

Diverse magnetic states have been reported for the martensite phase of Ni–Mn–X (X = In, Sn, Sb) based Heusler alloys, such as paramagnetic, superparamagnetic, antiferromagnetic, ferrimagnetic, ferromagnetic (FM) phases, two-phase mixtures and spin glass states [14–18]. This raises the interesting question of how the magnetic and ferroelastic properties interact. The origin of divergence between zero-field-cooling (ZFC) and field-cooling (FC) curves slightly below the Curie temperature of martensite state in almost all Ni–Mn–X (X = In, Sn, Sb) Heusler alloys has not been completely understood, though a number of possible mechanisms were proposed. [7, 15, 18–21] For instance, Gigla *et al* [22] and Ma *et al* [20] attributed splitting of magnetic ZFC/FC curves to spin disorder induced by excess magnetic atoms, e.g. Ni in martensite. The results of other work [18, 23] have implied that the excess magnetic atoms such as Co in Ni–(Co)–Mn–X (X = In, Sn, Sb) did not necessarily lead to the divergence between ZFC and FC curves, however. An alternative key factor might be the presence of ferroelastic twin walls of the martensite phase.

In this work, data from RUS, DC and AC magnetization and differential scanning calorimetry firstly show that $Ni_{50}Mn_{34}In_8Ga_8$ alloy undergoes phase transitions in the sequence, paramagnetic austenite → paramagnetic martensite → ferromagnetic martensite at ∼335 and ∼260 K, during cooling. Divergence between ZFC and FC curves below ∼220 K can be explained in terms of the development of a frustrated magnetic glass state in the ferromagnetic martensite. Correlation of a peak in acoustic loss with a peak in magnetic loss at ∼160 K is due to the effect of freezing of ferroelastic twin walls in giving rise to a further glassy magnetic transition. In addition, disrupting the martensitic structure by deforming the sample with a uniaxial force of 10 kN at room temperature can dilute the observed frustrated magnetic glass at 160–220 K in unstrained samples to a spin glass state.

A schematic unit cell of the parent cubic structure of NiMnInGa8 ($L2_1$, space group $Fm\bar{3}m$) is shown in the supplementary material (inset of figure S1) (stacks.iop.org/JPhysCM/32/325402/mmedia). There are four sites in the $L2_1$ unit cell, i.e., A (0, 0, 0), B (1/4, 1/4, 1/4), C (1/2, 1/2, 1/2), D (3/4, 3/4, 3/4) [24]. For NiMnInGa8 alloys, Ni atoms occupy *A* and *C* sites, while Mn occupies *B* sites and partially fills *D* sites. Other *D* sites are occupied by In and Ga atoms.

2. Experimental methods

$Ni_{50}Mn_{34}In_8Ga_8$ (NiMnInGa8 hereafter) ingots were prepared by arc melting of high-purity Ni(99.9%, T-metals), Mn(99.9%, T-metals), In(99.9%, T-metals) and Ga(99.9%, T-metals) with electromagnetic stirring in an argon atmosphere. They were then sealed in an evacuated silica tube and annealed at 1073 K for 48 h in order to improve chemical homogeneity, followed by quenching in air. A differential scanning calorimeter (DSC, TA Instruments Q-200) was used to detect the structural transition. A physical properties measurement system (PPMS Quantum Design) was used for vibrating sample magnetometer and AC magnetic susceptibility tests. Details of the RUS technique have been given in references [25–27]. Selected peaks in the RUS spectra were fitted with an asymmetric Lorentzian function using the software package Igor (WaveMetrics) to determine the resonance peak frequency, f, and width at half maximum height, Δf. The elastic constants scale with f^2 and the inverse mechanical quality factor, taken here as $Q^{-1} = \Delta f/f$, is a measure of acoustic loss. In a polycrystalline sample, f^2 scales primarily with the shear modulus because the predominant resonance motions involve shearing. Only a relatively small contribution is due to breathing motion, and hence to the bulk modulus, for most resonances.

3. Experimental results and discussion

Figure 1(a) shows a stack of RUS spectra collected in the temperature range 10–300 K and frequency range 0.1–1.2 MHz. Individual spectra, with amplitude in volts, have been displaced up the *y*-axis in proportion to the temperature at which they were collected, and the axis then labelled as temperature. Temperature dependent f^2 and Q^{-1} data obtained by fitting of the resonance peak near 0.46 MHz at room temperature are given for the entire temperature range, 10–450 K, as shown in figure 1(b). With falling temperature from ∼450 K, f^2 (∝shear modulus) first softened and then stiffened, resulting in a dip near 335 K. There is a hysteresis of ∼5 K between

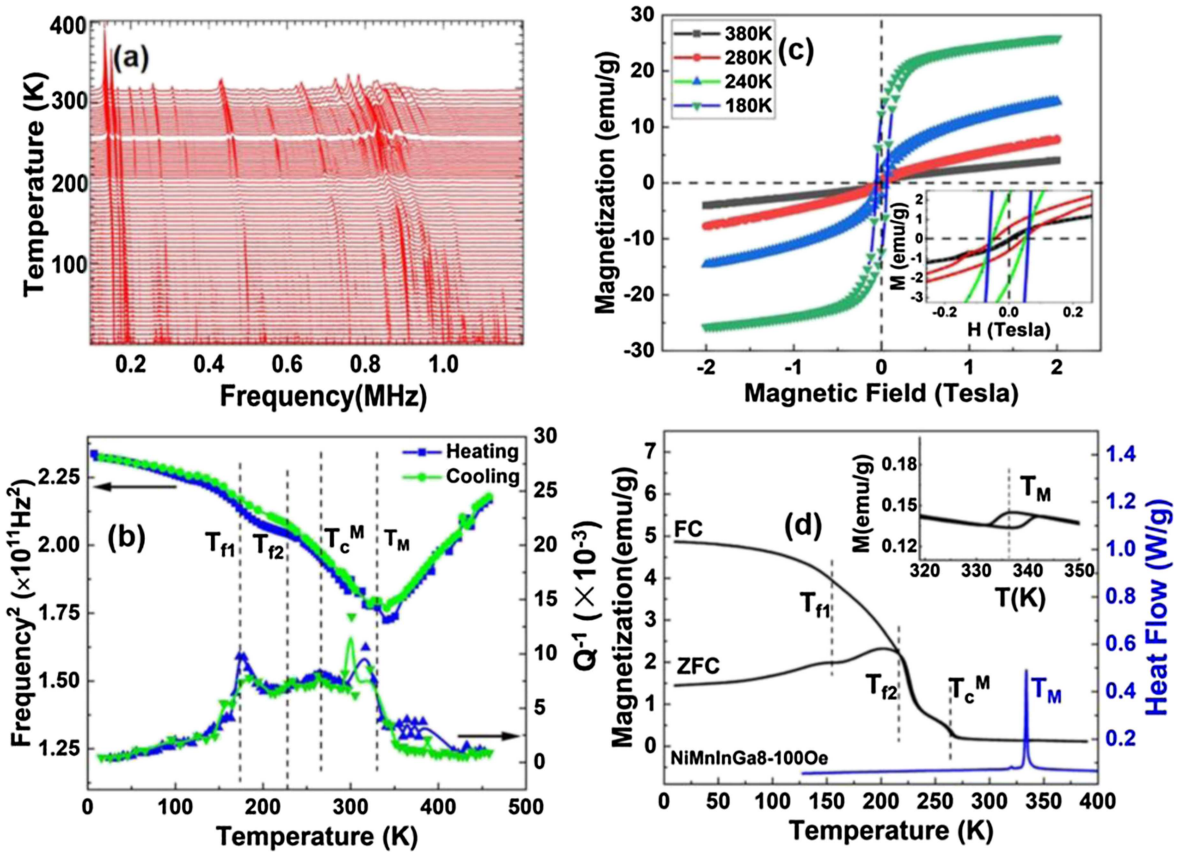

Figure 1. (a) RUS spectra of NiMnInGa8 alloy in the temperature interval 10–300 K collected in a heating sequence. (b) Temperature dependence of f^2 (left axis) and Q^{-1} (right axis) of the resonance peak with frequency near 0.46 MHz at room temperature. (c) M–H loops for NiMnInGa8 in the range ±2 T, at four selected temperatures. The inset in (c) shows magnified segments of M–H loops in the field range −0.3–+0.3 T. (d) ZFC/FC M–T data measured in a field of 100 Oe (black lines, left axis) and DSC data (blue line, right axis) for NiMnInGa8. T_c^M = Curie temperature of martensite, T_M = martensite transition temperature. The inset in (d) shows the magnified ZFC/FC curves measured in a field of 100 Oe through the temperature range 320–350 K.

cooling and heating for the minimum point of f^2 (∼335 K during cooling, ∼340 K during heating). Further confirmation of this being the martensitic transition is provided by the sharp peak in heat flow (blue curve in figure 1(d)). Steep non-linear softening of the shear modulus as the transition is approached from below and above is characteristic of a pseudoproper ferroelastic transition, which has bilinear coupling between a symmetry-breaking shear strain e and the driving order parameter Q. The formalities of how this coupling leads to the observed pattern have been set out in full in the literature (see, for example, [28]). The structural/electronic order parameter, Q_E, has the symmetry properties of irreducible representation Γ_3^+ of the parent $L2_1$ cubic state with space group $Fm\bar{3}m$ and couples bilinearly with tetragonal and orthorhombic shear strains, i.e., as λeQ [7, 8, 29]. Here, softening and stiffening of the combination of elastic constants C_{11}–C_{12} arises by bilinear coupling between Q_E and the symmetry breaking shear strain of DO_{22}-type tetragonal state (space group $I4/mmm$, confirmed by the diffraction pattern shown in figure S1). This is different from terms for strain coupling with the ferromagnetic order parameter, M, that are linear/quadratic, λeM^2, and biquadratic, λe^2M^2 [8, 24], and would give different patterns of elastic softening.

With respect to anelastic dissipation, the austenitic phase at $T > T_M$ gave low values of Q^{-1}, but displayed a steep increase from ∼10–20 K ahead of the martensitic transition (figure 1(b)). The increase is related to the precursor dynamics but would also be affected by the mobility of interfaces between coexisting austenite and martensite near T_M. In the stable martensitic state ($T < T_M$), a plateau of high anelastic loss, $Q^{-1} \approx 0.008$, persisted until the peak in Q^{-1} near 160 K, below which the Q^{-1} values returned to those of the parent austenite. This mirrors the classic pattern below a ferroelastic phase transition, in which high loss is due to the mobility of twin walls in an effectively viscous medium followed by Debye freezing or pinning of the walls at lower temperature, as marked by a peak in Q^{-1} and a small increase in elastic stiffness. For example, it is closely similar to the pattern shown by $Ni_{50}Mn_{35}In_{15}$ [7].

Conventional M–H loops in figure 1(c) show that the austenite phase exhibits near-zero hysteresis at 380 K, with low remnant and saturation magnetizations. It is thus considered to be paramagnetic. At 280 K ($T_c^M < T < T_M$), M–H data still show low saturation and remnant magnetization values, corresponding to a paramagnetic martensite state. The M–H loops at 240 K and 180 K ($T < T_c^M$) show that the martensite has become more ferromagnetic upon cooling. No premarten-

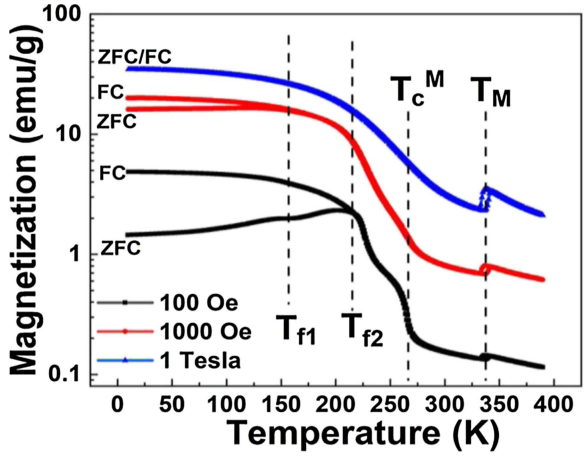

Figure 2. ZFC/FC M–T curves of NiMnInGa8 measured in fields of 100 Oe, 1 kOe and 1 T (10 kOe) through the temperature interval 10–390 K.

sitic transition was observed in the austenitic phase above T_M, which is different from previously reported Ni–Mn–Ga alloys [30–33]. The phase transition sequence in NiMnInGa8 is therefore paramagnetic austenite ($L2_1$, space group $Fm\bar{3}m$) → paramagnetic martensite (DO_{22}, space group $I4/mmm$) → ferromagnetic martensite. Diffraction data show persistence of some of the parent austenite down to room temperature (supplementary material, figure S1).

ZFC/FC splitting behaviour observed in the temperature range 10–220 K under different magnetic fields is shown in figures 1(d) and 2. The ZFC measurements were made during heating from 10 to 390 K in a field of 100 Oe, 1 kOe or 1 T following cooling in zero field. FC measurements were made during cooling back to 10 K with the same field as had been applied during heating, i.e. 100 Oe, 1 kOe or 1 T. There was a weak anomaly in the magnetic moment at T_M ∼335 K, the amplitude of which increased with increasing field. The transition temperature did not overtly shift between 100 Oe and 1 T. Divergence between the ZFC and FC curves at 100 Oe occurred at $T_{f2} \approx 220$ K, indicating the start of irreversibility for the magnetic state of the martensite phase below the ferromagnetic transition temperature of martensite $T_c{}^M = 260$ K. The divergence became smoothed out when the measuring field was increased to 1000 Oe and 1 T and the divergence temperature of ZFC/FC reduced with increasing field (figure 2). These two features are attributed to the development of a frustrated magnetic glass state in ferromagnetic martensite [15, 20, 23, 34, 35]. There is then another weak anomaly near 160 K in the low field data, labelled here as T_{f1}.

Figure 3(a) shows the temperature dependence of real, χ', and imaginary, χ'', parts of the AC susceptibility measured at a single frequency of 111 Hz with the DC field set at 100 Oe and the amplitude of the AC field set at 5 Oe. A weak shoulder appearing at ∼260 K in the χ'–T curve is ascribed to the magnetic transition of martensite ($T_c{}^M$). The sharp peak in χ' at ∼220 K (T_{f2}) was accompanied by a sharp peak in χ''. There is then a broad, much weaker peak in both χ' and χ'' at ∼160 K (T_{f1}). A close analogue, in terms of structure and chemistry, is $Ni_{50}Mn_{35}In_{15}$, in which a paramagnetic to ferromagnetic transition in the martensitic phase starts at ∼200 K, followed by bifurcation of FC and ZFC DC magnetization curves at a slightly lower temperature attributed to the presence of a spin-glass-like state [7]. Khovaylo *et al* [15] referred to the glassy magnetic state which develops below T_c^M in $Ni_{50}Mn_{34.8}In_{15.2}$ as a cluster glass. Neither of these two Heusler alloys showed the additional weak anomaly reported here at T_{f1} for NiMnInGa8, however. This seems to be more like the magnetic behaviour shown by $Ni_{48}Co_2Mn_{38}Sb_{12}$ which has a glassy magnetic freezing temperature at ∼130 K (T_{f1}) which is well below the FC/ZFC bifurcation temperature (T_{f2}) of ∼254 K.

Figures 3(b) and (c) show the results of AC magnetic measurements in a 100 Oe DC field with a 5 Oe AC field at frequencies of 9, 19, 199 and 999 Hz, before and after the sample was deformed in a hydropress. The unstrained sample, with mass 64.6 mg and thickness ∼0.8 mm, was subject to a uniaxial force of 10 kN until its thickness was reduced to ∼0.48 mm, corresponding to a strain of ∼40%. The force was released prior to new magnetic measurements being made. Further DSC data and M–T data (supplementary material, figures S2 and S3) confirmed that the martensitic transition still occurred at ∼340 K in the deformed sample. Values of the fitted empirical parameter $\Phi = \Delta T_f/(T_f \Delta \log_{10} f)$ at T_{f1} and T_{f2} of unstrained samples were found to be ∼0.004 and ∼0.005, respectively, which are closer to the reported values of magnetic (spin) glass, 0.005–0.02, than to the value of ∼0.1 for the blocked superparamagnetic state [18, 20]. This further supports the arguments for glassy magnetic behaviour at T_{f1} and T_{f2} in NiMnInGa8. The temperature-dependent AC magnetic properties of deformed samples (figure 3(c)) were markedly different from those of the as-grown, unstrained samples (figure 3(b)). In particular, the χ' and χ'' peaks at T_{f2} of unstrained samples almost disappeared from measurements on the deformed sample. The T_{f1} peak became stronger for strained NiMnInGa8 alloy and shifted to higher (∼175 K) and lower (∼150 K) temperature on χ'–T and χ''–T curves, respectively. The value of Φ around the frequency-dependent T_{f1} peak of strained samples is ∼0.014, indicative of a slowing-down spin glass state.

Following Nayak *et al* [23], the frequency dispersion in χ'–T curves through T_{f1} of the strained NiMnInGa8 sample was analysed using the empirical Vogel–Fulcher law $\omega = \omega_0 \exp\left(-E_a/k_B\left(T_g(\omega) - T_0\right)\right)$, as shown in the figure 3(d). E_a is an activation energy, k_B is the Boltzmann constant, $T_g(\omega)$ is the glass freezing temperature at measuring frequency ω, and T_0 is the glass freezing temperature for $\omega = 0$ Hz [36, 37]. The best fit to the data gave $T_0 \sim 169$ K, $\omega_0 \sim 10^5$ s^{-1} and $T_g/T_0 \sim 1.05$, which is viewed as additional evidence for a spin-glass-like transition [36, 38].

The complex glassy magnetic behaviour at T_{f1} and T_{f2} in the ferromagnetic martensite phase of NiMnInGa8 provides an illuminating comparison with the acoustic relaxation data from RUS. Although the measuring frequencies were different, freezing of the ferroelastic domain walls appears to be more or less coincident with the glassy magnetic freezing

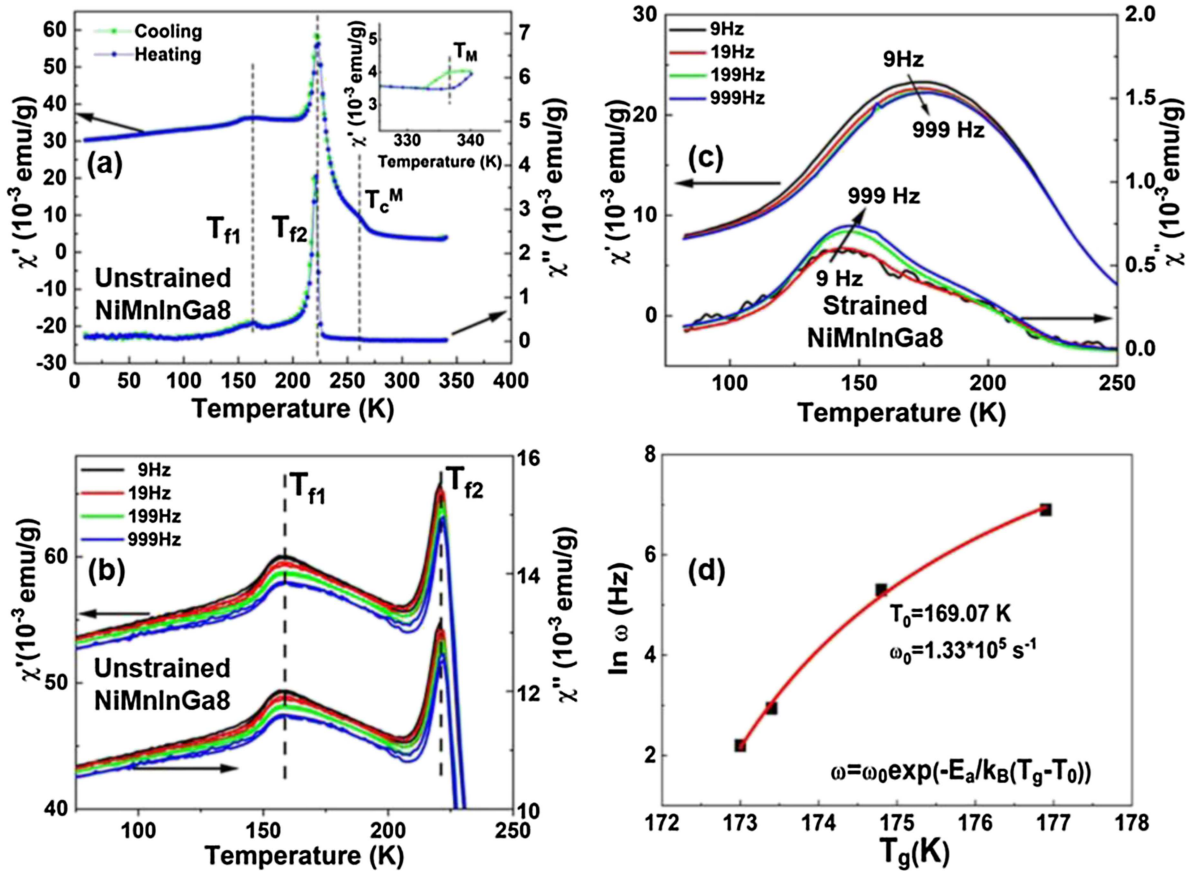

Figure 3. (a) Variation of the real part (χ') and imaginary part (χ'') of AC magnetic susceptibility at a single frequency of 111 Hz in the temperature range 10–340 K for unstrained $Ni_{50}Mn_{34}In_8Ga_8$. (b), (c) Frequency dependence (9, 19, 199, 999 Hz) of χ'–T and χ''–T curves for the as-grown (unstrained) sample and the sample strained under a load of 10 kN. (d) Fitting results of the frequency dependence of the temperatures ($T_g(\omega)$) of strained samples at which there were maxima in χ', using the Vogel–Fulcher relation $\omega = \omega_0 \exp\left(-E_a/k_B\left(T_g(\omega) - T_0\right)\right)$.

behaviour seen at T_{f1}, implying that the two processes are interdependent. As suggested in previous work [14–18, 20], some ferroelastic variants of martensite in Ni–Mn–X (X = In, Sn, Sb) Heusler alloys couple with magnetic clusters below T_c^M. If there is any magnetoelastic coupling, local strain variations associated with ferroelastic interaction between randomly oriented martensite variants below T_c^M must influence the mobility of the coupled magnetic domain walls to some extent. Freezing of the ferroelastic domain walls could then give rise to freezing of the magnetic domain walls or clusters and would imply that the glassy magnetic behaviour at T_{f1} relates specifically to glassy freezing of magnetic moments within or close to the ferroelastic twin walls.

Although the resulting microstructure of the deformed sample was not characterized, it is well understood that plastic deformation of martensite is accommodated via dislocations and deformation twinning. Magnetic ordering in the deformed sample will therefore have been strongly influenced by a high density of dislocations and pinned/interacting twin walls, which would account for the extra spin disorder. An additional contribution to spin disorder might have come from local changes to Mn(4b)–Mn(4b) and Mn(4b)–Mn(4d) distances, which are believed to influence magnetic exchange interactions in Ni–Mn–Fe–In alloys [15].

4. Conclusions

In summary, the transition sequence of the NiMnInGa8 alloy during cooling has been determined by resonant ultrasound spectroscopy, DC and AC magnetization and differential scanning calorimetry. The divergence of ZFC/FC curves is ascribed to magnetic frustration/disorder in the martensite phase. Correlation between acoustic and AC magnetic measurements suggests that magnetic glassy freezing are coupled with strain variations associated with the presence and relaxation dynamics of ferroelastic twin walls at lower temperature or external fields.

Acknowledgments

The authors gratefully acknowledge the financial support of the China Scholarship Council (Grant No. 201506280034), National Natural Science Foundation of China (Grant Nos. 51831006, 51431007, 51621063, 51772238), as well as Program for Changjiang Scholars and Innovative Research Team in University (IRT_17R85). RUS facilities in Cambridge University have been funded by the Natural Environment Research Council and the Engineering and Physical Sciences Research Council of Great Britain (Grant Nos. NE/B505738/1, NE/F017081/1, EP/I036079/1).

ORCID iDs

Sen Yang https://orcid.org/0000-0002-3802-8020
Michael A Carpenter https://orcid.org/0000-0003-2855-0007

References

[1] Carpenter M 2015 Static and dynamic strain coupling behaviour of ferroic and multiferroic perovskites from resonant ultrasound spectroscopy *J. Phys.: Condens. Matter* **27** 263201
[2] Yang S, Bao H, Zhou C, Wang Y, Ren X, Matsushita Y, Katsuya Y, Tanaka M, Kobayashi K, Song X and Gao J 2010 Large magnetostriction from morphotropic phase boundary in ferromagnets *Phys. Rev. Lett.* **104** 197201
[3] Liu W and Ren X 2009 Large piezoelectric effect in Pb-free ceramics *Phys. Rev. Lett.* **103** 257602
[4] Kainuma R, Imano Y, Ito W, Sutou Y, Morito H, Okamoto S, Kitakami O, Oikawa K, Fujita A and Kanomata T 2006 Magnetic-field-induced shape recovery by reverse phase transformation *Nature* **439** 957
[5] Sozinov A, Likhachev A A, Lanska N and Ullakko K 2002 Giant magnetic-field-induced strain in NiMnGa seven-layered martensitic phase *Appl. Phys. Lett.* **80** 1746
[6] Ghorbani Zavareh M, Salazar Mejía C, Nayak A K, Skourski Y, Wosnitza J, Felser C and Nicklas M 2015 Direct measurements of the magnetocaloric effect in pulsed magnetic fields: the example of the Heusler alloy $Ni_{50}Mn_{35}In_{15}$ *Appl. Phys. Lett.* **106** 071904
[7] Mejía C S, Nayak A K, Schiemer J A, Felser C, Nicklas M and Carpenter M A 2015 Strain behavior and lattice dynamics in $Ni_{50}Mn_{35}In_{15}$ *J. Phys.: Condens. Matter* **27** 415402
[8] Salazar Mejía C, Born N O, Schiemer J A, Felser C, Carpenter M A and Nicklas M 2018 Strain and order-parameter coupling in Ni-Mn-Ga Heusler alloys from resonant ultrasound spectroscopy *Phys. Rev.* B **97** 094410
[9] Zhang L, Ren X and Carpenter M A 2017 Influence of local strain heterogeneity on high piezoelectricity in $0.5Ba(Zr_{0.2}Ti_{0.8})O_3$-$0.5(Ba_{0.7}Ca_{0.3})TiO_3$ ceramics *Phys. Rev.* B **95** 054116
[10] Salje E K H, Carpenter M A, Nataf G F, Picht G, Webber K, Weerasinghe J, Lisenkov S and Bellaiche L 2013 Elastic excitations in $BaTiO_3$ single crystals and ceramics: mobile domain boundaries and polar nanoregions observed by resonant ultrasonic spectroscopy *Phys. Rev.* B **87** 014106
[11] Schiemer J, Carpenter M A, Evans D M, Gregg J M, Schilling A, Arredondo M, Alexe M, Sanchez D, Ortega N, Katiyar R S, Echizen M, Colliver E, Dutton S and Scott J F 2014 Studies of the room-temperature Multiferroic $Pb(Fe_{0.5}Ta_{0.5})_{0.4}(Zr_{0.53}Ti_{0.47})_{0.6}O_3$: resonant ultrasound spectroscopy, dielectric, and magnetic phenomena *Adv. Funct. Mater.* **24** 2993
[12] Goncalves-Ferreira L, Redfern S A T, Artacho E and Salje E K H 2008 Ferrielectric twin walls in $CaTiO_3$ *Phys. Rev. Lett.* **101** 097602
[13] Scott J F, Bryson J, Carpenter M A, Herrero-Albillos J and Itoh M 2011 Elastic and anelastic properties of ferroelectric $SrTi^{18}O_3$ in the kHz-MHz regime *Phys. Rev. Lett.* **106** 105502
[14] Nayak A K, Nicklas M, Chadov S, Khuntia P, Shekhar C, Kalache A, Baenitz M, Skourski Y, Guduru V K, Puri A, Zeitler U, Coey J M D and Felser C 2015 Design of compensated ferrimagnetic Heusler alloys for giant tunable exchange bias *Nat. Mater.* **14** 679
[15] Khovaylo V V, Kanomata T, Tanaka T, Nakashima M, Amako Y, Kainuma R, Umetsu R Y, Morito H and Miki H 2009 Magnetic properties of $Ni_{50}Mn_{34.8}In_{15.2}$ probed by Mössbauer spectroscopy *Phys. Rev.* B **80** 144409
[16] Aksoy S, Acet M, Deen P P, Mañosa L and Planes A 2009 Magnetic correlations in martensitic Ni-Mn-based Heusler shape-memory alloys: Neutron polarization analysis *Phys. Rev.* B **79** 212401
[17] Wang B M, Liu Y, Ren P, Xia B, Ruan K B, Yi J B, Ding J, Li X G and Wang L 2011 Large exchange bias after zero-field cooling from an unmagnetized state *Phys. Rev. Lett.* **106** 077203
[18] Cong D Y, Roth S and Schultz L 2012 Magnetic properties and structural transformations in Ni–Co–Mn–Sn multifunctional alloys *Acta Mater.* **60** 5335
[19] Chatterjee S, Giri S, De S K and Majumdar S 2009 Reentrant-spin-glass state in $Ni_2Mn_{1.36}Sn_{0.64}$ shape-memory alloy *Phys. Rev.* B **79** 092410
[20] Ma L, Wang W H, Lu J B, Li J Q, Zhen C M, Hou D L and Wu G H 2011 Coexistence of reentrant-spin-glass and ferromagnetic martensitic phases in the $Mn_2Ni_{1.6}Sn_{0.4}$ Heusler alloy *Appl. Phys. Lett.* **99** 182507
[21] Tian F, Cao K, Zhang Y, Zeng Y, Zhang R, Chang T, Zhou C, Xu M, Song X and Yang S 2016 Giant spontaneous exchange bias triggered by crossover of superspin glass in Sb-doped $Ni_{50}Mn_{38}Ga_{12}$ Heusler alloys *Sci. Rep.* **6** 30801
[22] Gigla M, Szczeszek P and Morawiec H 2006 The structure of non-stoichiometric alloys based on Ni_2MnGa *Mater. Sci. Eng.* A **438–440** 1015
[23] Nayak A K, Suresh K G and Nigam A K 2011 Correlation between reentrant spin glass behavior and the magnetic order–disorder transition of the martensite phase in Ni-Co-Mn-Sb Heusler alloys *J. Phys.: Condens. Matter* **23** 416004
[24] Kataoka M, Endo K, Kudo N, Kanomata T, Nishihara H, Shishido T, Umetsu R Y, Nagasako M and Kainuma R 2010 Martensitic transition, ferromagnetic transition, and their interplay in the shape memory alloys $Ni_2Mn_{1-x}Cu_xGa$ *Phys. Rev.* B **82** 214423
[25] McKnight R E A, Carpenter M A, Darling T W, Buckley A and Taylor P A 2007 Acoustic dissipation associated with phase transitions in lawsonite, $CaAl_2Si_2O_7(OH)_2{\cdot}H_2O$ *Am. Mineral.* **92** 1665
[26] Migliori A, Sarrao J L, Visscher W M, Bell T M, Lei M, Fisk Z and Leisure R G 1993 Resonant ultrasound spectroscopic techniques for measurement of the elastic moduli of solids *Physica* B **183** 1
[27] McKnight R E A, Moxon T, Buckley A, Taylor P A, Darling T W and Carpenter M A 2008 Grain size dependence of elastic anomalies accompanying the α–β phase transition in polycrystalline quartz *J. Phys.: Condens. Matter* **20** 075229
[28] Carpenter M A and Salje E K 1998 Elastic anomalies in minerals due to structural phase transitions *Eur. J. Mineral.* **10** 693
[29] Carpenter M A and Howard C J 2018 Fundamental aspects of symmetry and order parameter coupling for martensitic transition sequences in Heusler alloys *Acta Crystallogr.* B **74** 560
[30] Sedlák P, Seiner H, Bodnárová L, Heczko O and Landa M 2017 Elastic constants of non-modulated Ni-Mn-Ga martensite *Scr. Mater.* **136** 20
[31] Chang S H and Wu S K 2008 Low-frequency damping properties of near-stoichiometric Ni2MnGa shape memory alloys under isothermal conditions *Scr. Mater.* **59** 1039
[32] Chernenko V A, Pons J, Seguí C and Cesari E 2002 Premartensitic phenomena and other phase transformations in Ni-Mn-Ga alloys studied by dynamical mechanical analysis and electron diffraction *Acta Mater.* **50** 53
[33] Pérez-Landazábal J I, Sánchez-Alarcos V, Gómez-Polo C, Recarte V and Chernenko V A 2007 Vibrational and magnetic

behavior of transforming and nontransforming Ni-Mn-Ga alloys *Phys. Rev.* B **76** 092101

[34] Li D X, Nimori S, Shiokawa Y, Haga Y, Yamamoto E and Onuki Y 2003 Ferromagnetic cluster glass behavior in U_2IrSi_3 *Phys. Rev.* B **68** 172405

[35] Wang Y T, Bai H Y, Pan M X, Zhao D Q and Wang W H 2006 Multiple spin-glass-like behaviors in a Pr-based bulk metallic glass *Phys. Rev.* B **74** 064422

[36] Sarkar S, Ren X and Otsuka K 2005 Evidence for strain glass in the ferroelastic-martensitic system $Ti_{50-x}Ni_{50+x}$ *Phys. Rev. Lett.* **95** 205702

[37] Zhang L, Lou X, Wang D, Zhou Y, Yang Y, Kuball M, Carpenter M A and Ren X 2017 Glass-Glass transitions by means of an acceptor-donor percolating electric-dipole network *Phys. Rev. Appl.* **8** 054018

[38] Lundgren L, Svedlindh P and Beckman O 1982 Experimental indications for a critical relaxation time in spin-glasses *Phys. Rev.* B **26** 3990